

FTIR spectroscopy of lawsonite between 82 and 325 K

EUGEN LIBOWITZKY AND GEORGE R. ROSSMAN

Division of Geological and Planetary Sciences, California Institute of Technology, 170-25, Pasadena, California 91125, U.S.A.

ABSTRACT

Lawsonite single crystals were investigated by polarized FTIR spectroscopy at wavenumbers between 8000 and 1000 cm^{-1} and temperatures between 82 and 325 K. This temperature range contains three lawsonite phases— $Cmcm > 273 \text{ K}$, $273 \text{ K} > Pm\bar{c}n > 150 \text{ K}$, $P2_1cn < 150 \text{ K}$ —which are characterized by different rotations of hydroxyl groups and H_2O molecules. Unlike previous studies of H_2O in minerals, which assumed weakly bonded, symmetric H_2O molecules, the highly asymmetric H_2O molecule in lawsonite required a modified approach that uses the single, uncoupled O-H stretching frequencies and orientations of the individual OH groups in the H_2O molecule.

The formation of a strong hydrogen-bond system with decreasing temperature is characterized by a shift of O-H stretching bands from 2968 and 3252 cm^{-1} at 325 K to 2817 and 3175 cm^{-1} at 82 K. These frequencies are in good agreement with the corresponding hydrogen-bond lengths ($\text{H}\cdots\text{O} = 1.66$ and 1.74 Å, $\text{O}-\text{H}\cdots\text{O} = 2.60$ and 2.66 Å) at low temperatures. The orientations of the O-H vectors determined from polarized IR measurements also confirm the H-atom positions refined from previous X-ray structure determinations at low temperatures. However, the disagreement between spectroscopically determined distances (and orientations) and those from X-ray refinements at ambient conditions indicates that the room-temperature $Cmcm$ structure of lawsonite contains dynamically disordered hydroxyl groups and H_2O molecules. The smooth changes of stretching and bending frequencies across the phase boundaries at 273 and 150 K also suggest that the lawsonite phase transitions are of a dynamic order-disorder type rather than a displacive type.

Deuteration experiments on differently oriented, single-crystal lawsonite slabs at 350 °C and 1.2–2.5 kbar showed that lawsonite has a preferred H-diffusion direction parallel to [001]. This is consistent with the crystal structure showing channels parallel to [001], which are solely occupied by H atoms. The spectra of isotopically diluted samples, which are almost identical to those of natural lawsonite, indicate that band-coupling effects are generally weak.

The FTIR powder spectra of the lawsonite-type mineral hennomartinite, $\text{SrMn}_2[\text{Si}_2\text{O}_7](\text{OH})_2\cdot\text{H}_2\text{O}$, are similar to the lawsonite Z spectra and confirm the existence of both strong and weak hydrogen bonds in its structure.

INTRODUCTION

Lawsonite, $\text{CaAl}_2[\text{Si}_2\text{O}_7](\text{OH})_2\cdot\text{H}_2\text{O}$, is a common constituent in rocks from high- P and low- T metamorphic environments like blueschists. The structure, which contains both discrete hydroxyl groups and H_2O molecules, was first solved by Wickman (1947) in the (incorrect) space group $C222_1$. After several subsequent investigations by different authors, Baur (1978) refined the structure in space group $Cm\bar{c}m$ and also roughly located the positions of the H atoms. Libowitzky and Armbruster (1995) refined the structures of lawsonite (including the exact H positions) at temperatures between 110 and 500 K. They found that lawsonite shows phase transitions at 273 and 150 K, mainly involving changes in the positions of the H atoms and their immediate neighbors, as well as

changes in the hydrogen-bond system. In the present paper the crystallographic setting is identical to that of Libowitzky and Armbruster (1995), i.e., $X // a$ (5.85 Å), $Y // b$ (8.79 Å), $Z // c$ (13.13 Å).

The room- T structure of lawsonite, $Cm\bar{c}m$ (Fig. 1a), consists of chains of edge-sharing AlO_6 octahedra parallel to [100], which are interconnected by Si_2O_7 groups. The remaining interstices of the framework are occupied by Ca atoms, H_2O molecules, and H atoms of hydroxyl groups. The H_2O molecules and hydroxyl groups are aligned parallel to the (100) plane, their H atoms being symmetrically related. They show weak hydrogen bonds to neighboring O4 and O2 atoms. Below 273 K the structure changes to space group $Pm\bar{c}n$, which is accompanied by the loss of the $\bar{c}n$ mirror plane (Fig. 1b). The H_2O groups rotate within the (100) plane, thus strengthening

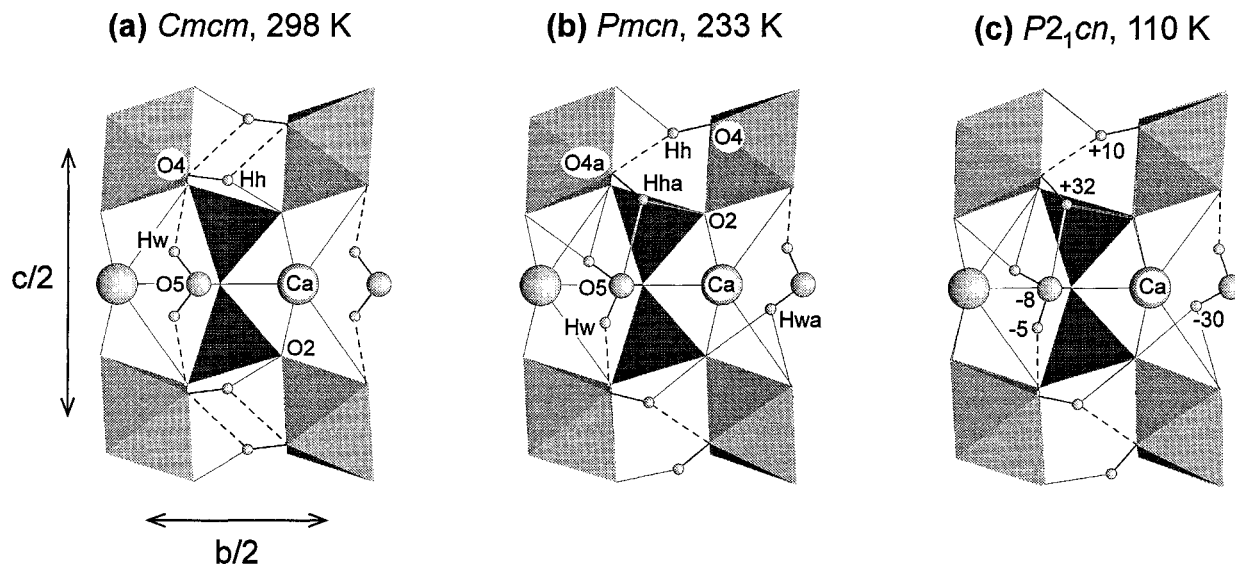


FIGURE 1. The structures of lawsonite projected along [100]. (a) $Cmcm$ at room temperature. (b) $Pmcn$ at 233 K. (c) $P2_1cn$ at 110 K. Numbers denote the deviation of the atom from the (100) plane ($x = 0$) in angstroms times 10^{-2} . Dashed lines indicate $H \cdots O$ bonds shorter than $2.00(2)$ Å.

one hydrogen bond to a neighboring O4 atom and weakening another to the other O4 atom. Similarly, the degree of rotation is different for each H atom of the hydroxyl groups, which increases the strength of one hydrogen bond and decreases the strength of the other. Below 150 K the structure changes to the polar space group $P2_1cn$, which is characterized by the loss of the m -mirror plane (Fig. 1c). In addition to a further strengthening of the strong hydrogen bonds, the weakly bonded Hwa atoms of the H_2O groups deviate downward from the former m -plane, and those of the hydroxyl groups (Hha) deviate upward.

Libowitzky and Armbruster (1995) also showed that the phase transitions are characterized by nonlinear changes in lattice parameters and optical constants. However, a recent study by Comodi and Zanazzi (1996), who investigated the structure and lattice parameters of lawsonite at high pressures and temperatures (deriving thermal expansion and compressibility coefficients), reported smooth, linear changes of lattice constants and atomic positional parameters.

An IR spectroscopic investigation of lawsonite by Labotka and Rossman (1974) determined the alignment of the H_2O and hydroxyl groups parallel to (100). Their 78 K spectra also showed a remarkable peak splitting, but at that time the low-temperature phases of lawsonite were unknown. Another IR and Raman spectroscopic investigation of lawsonite (Le Cléac'h and Gillet 1990) focused on the lattice vibrations and their assignment.

The aim of the present paper is to compare the temperature-dependent structural changes with the IR-active stretching and bending frequencies of the H_2O and hydroxyl groups and to reconcile band frequencies with hydrogen-bond distances, and polarized band intensities with geometric H-site information. A further objective was to

obtain additional knowledge about the quantitative behavior of IR bands at different absorption frequencies.

EXPERIMENTAL METHODS

The present investigation used several crystals of lawsonite from Reed Ranch, Tiburon, California, with well-developed crystal faces and up to 1 cm in size. The samples were provided by the Museum of Natural History, Bern, Switzerland (sample NMBE A7331), and the California Institute of Technology. They were milky white to transparent with a blue tint (strongest parallel to [100]). In some cases the rims of the crystals contained abundant chlorite inclusions. However, even though large, clear crystals of lawsonite were not available, small and thin regions of the crystals were almost free from fissures and inclusions.

Sample preparation

Because the preparation of extremely thin, oriented crystal slabs was a major part of the present work, it is described thoroughly. Crystals were oriented according to their morphology [pinacoid (001) with striations parallel to [100] and prism (110)] and checked by optical microscopy. They were cut on a low-speed diamond-wheel saw parallel to (100), (010), and (001) into slices of ~ 500 μm thickness. The accuracy of the orientation is considered to be $\pm 2^\circ$. However, even a misorientation of $\pm 5^\circ$ would not show significant effects on the polarized spectra (Libowitzky and Rossman 1996). Each slab (2–5 mm in size) was ground manually on one side with 30, 15, and 9 μm Al_2O_3 grinding films and finally polished with 6 and 1 μm diamond films and 0.3 μm alumina film (3M). The polished side of each individual slab was then glued to a round microscope glass slide with the use of Aremco

Crystal Bond 509, which is an acetone-soluble adhesive. The glass slide with the attached crystal was mounted in a locally constructed sample holder to maintain flat and parallel grinding. The slab was then carefully ground by hand with 30, 15, and 9 μm alumina grinding films. The thickness was frequently checked with an electronic micrometer with an accuracy of 1 μm . Although a thickness of 150 μm was sufficient for the measurement of the moderate absorptions parallel to [100] (= X), a thickness of only 10 μm proved to be too much for the intense bands of the Y and Z spectra. Thus, crystals were ground to a thickness of ~ 10 μm with 9 μm alumina films. The final thicknesses of 3 and 4 μm were obtained by hand polishing the glass slide with the attached 10 μm crystal slab on a soft polishing cloth (Nylon, Buehler) with 1 μm alumina powder (Micropolish, Buehler). This final procedure produced rounded edges, but the central parts of the slab remained flat. The adhesive was then removed by soaking in acetone to obtain the unsupported crystal slice.

The success rate of this process is low. Only one 3 μm thick slab, one 4 μm thick slab, and five 10 μm thick slabs were recovered from approximately 25 starting slabs (many slabs were lost by grinding to "zero" or by attempting to remove the final plates from the glass slide). However, the unsupported slabs are superior to crystal slabs glued to a carrier material (as used in most single-crystal IR investigations of H_2O -rich materials), which show interfering bands from the adhesive (usually in the 2900–3000 cm^{-1} range).

FTIR spectroscopy

Polarized spectra were recorded on a Nicolet 60SX FTIR spectrometer. Although a Nicolet FTIR microscope was available, samples were measured in the standard sample compartment of the spectrometer, thus providing almost parallel beam conditions. For the measurements between 82 and 325 K a commercial cryocell (MMR technologies) using the Joule-Thompson effect (cooling by expansion of compressed nitrogen gas) was used. The absolute temperature accuracy was better than ± 2 K. During data acquisition, temperatures were kept constant to ± 0.5 K. The cell was equipped with polycrystalline CaF_2 windows and was evacuated to < 1 mtorr. The diameter of the measuring field was restricted by a 200 μm aperture. A liquid-nitrogen-cooled HgCdTe detector and a CaF_2 beam splitter were used for all measurements. For polarized spectra between 8000 and 2000 cm^{-1} , a water-cooled tungsten light source and an LiIO_3 crystal polarizer with an extinction ratio (I_{crossed} to I_{parallel}) better than 1:10000 were used. To observe the H_2O bending mode near 1600 cm^{-1} a water-cooled glowbar light source and an AgBr gold-wire grid polarizer (extinction ratio at 1600 cm^{-1} better than 1:100) were employed. A nominal resolution of 2 cm^{-1} was considered to be adequate for the acquisition of the sharp high-energy bands at low temperatures. To improve the S/N ratio, all spectra were averaged from at least 1024 single scans. The peak decomposition of the spectra and the exact deter-

mination of absorption frequencies and intensities were accomplished with the PeakFit software package (JANDEL Scientific) and the use of Voigt-shaped curves as a compromise between the spectroscopic Lorentz function and the statistical Gaussian function. Trials with modified, nonsymmetrical Gaussian functions (Sunshine et al. 1990) proved to be inappropriate for the fit of single bands. Unfortunately, low-frequency interference fringes caused by the extremely thin, doubly polished samples could not be removed by FFT filtering or by curve fitting with variable sine curves, neither in energy nor in wavelength units. Probably, the refractive indices (influencing the periodicity of the interference fringes) were strongly altered in the region of the strong absorbance bands between 4000 and 2500 cm^{-1} . Hence, intensity data are less accurate than might be expected from the smooth spectra.

Deuteration experiments

Doubly polished lawsonite slabs between 60 and 200 μm thick were used in deuteration experiments. The samples and at least the tenfold volume of D_2O were loaded into gold capsules, which were sealed by welding. The capsules were inserted into cold-seal pressure vessels and run at a temperature of 350 $^\circ\text{C}$ and D_2O pressures between 1.2 and 2.5 kbar (using Ar gas as pressure medium) for durations of 3.5–14 d. After the experiments the capsules were punctured with a needle to test for loss of D_2O . The deuterated sample surfaces appeared rough, indicating that some material had been dissolved in D_2O . A 7 d experiment at 400 $^\circ\text{C}$ showed tiny (100 μm) crystals of a new phase (probably anorthite) growing on the faces and edges of the lawsonite slabs. This behavior is in good agreement with the results of Pawley (1994) and Newton and Kennedy (1963), who determined the stability limits of lawsonite. The limiting boundary, which approaches extremely high pressures at moderate temperatures (e.g., 650 $^\circ\text{C}$, 25 kbar) prohibits faster deuteration experiments at higher temperatures.

RESULTS

FTIR spectra

The X , Y , and Z spectra of lawsonite are plotted in Figure 2 for temperatures between 82 and 325 K. The spectra are divided into the wavelength range 1400–1800 cm^{-1} , showing the H_2O bending mode, and the range 2500–3700 cm^{-1} , showing the O-H stretching modes of the hydroxyl and H_2O groups. The X spectrum is extended to 4900 cm^{-1} to show also the 4400 cm^{-1} metal–O–H motions. The spectra are in good agreement with those of Labotka and Rossman (1974) but reveal more details because of the use of unsupported crystal slabs and a modern FTIR spectrometer with a highly sensitive detector. In addition, the high-energy stretching bands appear much sharper and more intense than in the previous paper, which is attributed to the use of an almost perfect crystal polarizer (Libowitzky and Rossman 1996).

In comparison with the Y and Z spectra of lawsonite,

the *X* spectra show very weak absorption bands. (Note that the spectra of Fig. 2a are acquired from a 150 μm slab, whereas those of the *Y* and *Z* directions are recorded from 3 and 4 μm slabs.) The high-energy stretching bands near 3500–3600 cm^{-1} (two bands at low temperatures) are much more intense than the low-energy stretching bands near 2800–2900 cm^{-1} (visible only as a very weak, broad band) and 3200 cm^{-1} (invisible). The *X* direction reveals an additional band near 4400 cm^{-1} , which is split at low temperatures. Except for the three spectra at the lowest temperatures no H_2O bending mode is visible near 1600 cm^{-1} .

The *Y* spectra (Fig. 2b) show a strong high-energy stretching mode that splits into two sharp bands at low temperatures. These bands shift slightly toward higher energies with decreasing temperature. The low-energy stretching mode is very broad at ambient temperatures and narrows and increases in peak height toward low temperatures. It shows a remarkable band shift toward lower energies with decreasing temperature. The *Y* spectrum shows an H_2O bending mode near 1600–1650 cm^{-1} , which also reveals a slight temperature shift. The exclusive appearance of this peak in the *Y* spectrum was used for the first determination of the orientation of the H_2O molecules in lawsonite by Labotka and Rossman (1974).

The *Z* spectra (Fig. 2c) show exactly the same frequencies and almost the same intensities of the high-energy stretching modes as the *Y* spectra. As in the *Y* direction spectra, the low-energy stretching band is broad at ambient temperatures and narrows and increases in peak height toward low temperatures. However, it shows a stronger peak shift toward low energies, and the absolute peak position occurs at much lower wavenumbers than the low-energy band in the *Y* spectrum. The region of the H_2O bending mode shows two weak bands near 1550–1600 and 1700 cm^{-1} (note the different scale in comparison with *Y*), which become more intense at low temperatures. Their assignment to H_2O bending modes was confirmed by deuteration. A weak combination (stretching plus bending) mode at $\sim 5180 \text{ cm}^{-1}$ is also visible in the *Z* spectrum.

The almost exclusive appearance of the stretching and bending modes parallel to *Y* and *Z* indicates that the hydroxyl groups and H_2O molecules are aligned parallel to the (100) plane, which was previously reported by Labotka and Rossman (1974). However, the precise band assignment and determination of the O-H vector orientations within the (100) plane need some discussion and revision (see Discussion section). Generally, the two high-energy bands occur at identical positions in the *Y* and *Z* spectra and have almost identical intensities in both directions. (Note that the absorbance scales in Figs. 2b and 2c were chosen to facilitate direct comparison of the 3 and 4 μm crystal plates.) Thus, their O-H vectors are aligned at $\sim 45^\circ$ to the *Y* and *Z* directions. In addition, there occur one low-energy stretching band exclusively in the *Y* direction and another stretching band at even lower energy exclusively in the *Z* direction. Thus, there is one

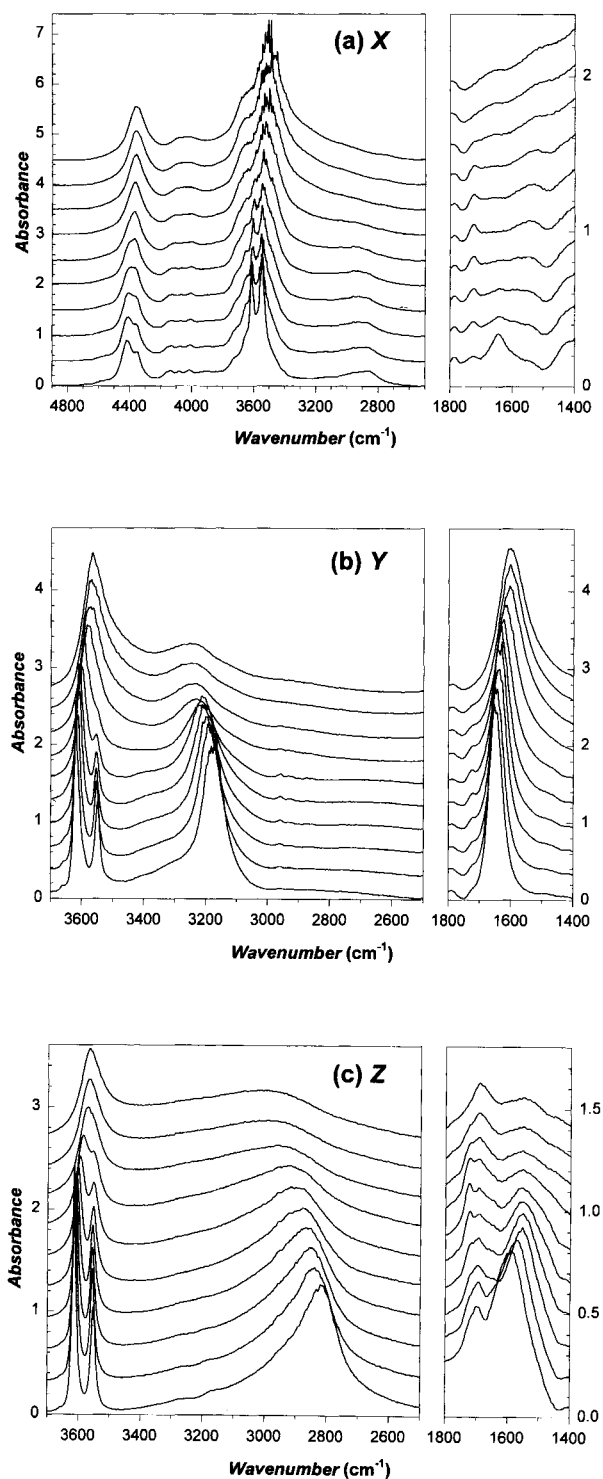


FIGURE 2. Polarized FTIR absorption spectra of lawsonite. (a) *X* spectra from a 150 μm (001) slab. (b) *Y* spectra from a 4 μm (001) slab and a 30 μm (100) slab (1800–1400 cm^{-1}). (c) *Z* spectra from a 3 μm (100) slab and a 30 μm (100) slab (1800–1400 cm^{-1}). Spectra are vertically offset by a constant value. Temperatures from bottom to top are 82, 110, 140, 165, 195, 225, 250, 275, 298, and 325 K.

TABLE 1. Hydrogen-bond distances (Å) in lawsonite

Space group T (K)	<i>P2₁cn</i> 110	<i>Pmcn</i> 155	<i>Pmcn</i> 233	<i>Cmcm</i> 295
Hw···O4	1.66	1.67	1.70	1.90
O5-Hw···O4	2.599	2.599	2.609	2.666
Hwa···O4a	2.41	2.24	2.22	1.90
O5-Hwa···O4a	2.777	2.770	2.749	2.666
Hwa···O2	2.20 (2.51)	2.32 (× 2)	2.33 (× 2)	2.43
O5-Hwa···O2	3.146 (3.182)	3.174 (× 2)	3.191 (× 2)	3.229
Hh···O4a	1.74	1.73	1.77	2.01
O4-Hh···O4a	2.660	2.677	2.705	2.752
Hh···O2	2.33 (2.48)	2.43 (× 2)	2.40 (× 2)	2.21
O4-Hh···O2	2.995 (2.976)	2.982 (× 2)	2.972 (× 2)	2.932
Hha···O2a	2.04 (2.55)	2.19 (× 2)	2.20 (× 2)	2.21
O4a-Hha···O2a	2.865 (2.941)	2.900 (× 2)	2.906 (× 2)	2.932
Hha···O5	2.14	2.20	2.16	>2.5
O4a-Hha···O5	2.777	2.770	2.749	2.666

Note: Refinement of data from Libowitzky and Armbruster (1995) with O-H distances constrained to 0.98(0) Å. Estimated standard deviations are ~2 in the last digit of all values. Symmetric bifurcation of hydrogen bonds is indicated by "×2" in parentheses. The values in parentheses in the 110 K data represent the distances to the O2b and O2c atoms, which formed the symmetrically bifurcated bonds in the *Pmcn* structure.

O-H vector aligned almost parallel to *Y* and another one parallel to *Z*.

Hydrogen-bond system

Table 1 presents important H···O and O-H···O distances in lawsonite. These data were gained from a refinement of the X-ray data sets of Libowitzky and Armbruster (1995) with the use of a bond-distance constraint of O-H = 0.98(0) Å, which represents a mean O-H distance from a variety of different hydrates (Franks 1973). The refinements were made with the SHELXTL program package (Siemens). Unlike the original values in Libowitzky and Armbruster (1995), which represent the actual electron densities but give very short O-H distances of 0.7 and 0.8 Å [owing to displaced electrons of the H atoms and to strong librational motions (Lager et al. 1987)], the present data seem to draw a more realistic picture of the hydrogen-bond system. They are also preferred to the distances from a single-crystal neutron refinement at room temperature, which also yield rather short O-H distances of ~0.9 Å as a result of strong libration of the H₂O and hydroxyl groups (George Lager, personal communication). However, because of the dynamic behavior of the H atoms, Figure 1a and Table 1 show only average centers of gravity or displacement, whereas the actual, time-resolved values are somewhat different, as will be discussed below.

Analysis of the hydrogen-bond system from elevated to low temperatures shows that in the *Cmcm* structure the (symmetric) H atoms of the H₂O molecules are only moderately bonded to their neighboring O atoms (Hw···O4 = 1.90 Å), even though the O5-Hw···O4 distance is rather short (2.67 Å). Figure 1a shows that the bonds are considerably bent. Below the transition temperature at 273 K, one hydrogen bond (Hw···O4) of the H₂O molecule is strengthened to distances as short as 1.66 Å in the *P2₁cn* structure. However, the O5-Hw···O4 is shortened

to only 2.60 Å, but the bond is almost straight at low temperatures (Figs. 1b and 1c). Because of the rotation of the H₂O molecule, the other hydrogen bonds (Hwa···O4a and Hwa···O2) become very weak in the low-temperature structures (2.20–2.41 Å).

The hydrogen bonds of the (symmetric) hydroxyl groups seem to be rather weak in the *Cmcm* structure (Hh···O4 = 2.01 Å), even though the O4-Hh···O4' (O4' is the symmetric equivalent of O4) distance is considerably short (2.75 Å). There is an additional, very weak, symmetric, bifurcated hydrogen bond (O2···Hh···O2') with an O···H length of 2.21 Å (Fig. 1a). Thus, considering this very weak bond, the bond system may be described as trifurcated. Below the 273 K transition temperature the Hh···O4a bond of one hydroxyl group is strengthened to values as short as 1.74 Å in the *P2₁cn* structure. The O4-Hh···O4a distance is slightly shortened to 2.66 Å, and the bond becomes straighter. The bifurcated Hh···O2 bonds are almost abandoned at low temperatures. The other hydroxyl group gives up the Hha···O4 bond, but (by rotation) forms an additional very weak bond to a neighboring O5 atom (Hha···O5 = 2.14–2.20 Å). The bifurcated bonds remain almost constant in the *Pmcn* structure, but one of them is enhanced to 2.04 Å in the *P2₁cn* structure.

Deuteration experiments

The aim of the deuteration experiments was to produce isotopically diluted samples, which should show reduced band-coupling effects and thus better resolution of the spectra (Franks 1973). The reduction of the amount of H₂O by D₂O substitution also facilitated the use of thicker crystal slabs, which reduced the preparative efforts enormously.

A preliminary, 3.5 d deuteration test on 60 μm (001) lawsonite slabs in a Teflon-lined digestion vessel at 150 °C resulted in only <1% exchange. The 3.5 d experiments on 200 μm (001) lawsonite slabs in cold-seal vessels at 350 °C and 1.2–1.3 kbar resulted in ~30% deuteration. An FTIR investigation of the outer 20 μm layer of one slab (parallel to *Y*) revealed ~80% deuteration (estimated by comparison of the intensities of OH bands in the deuterated sample to the band intensities of pure H lawsonite). A 4 d experiment at 400 °C and 1.2–1.3 kbar resulted in ~50% deuteration. To obtain *Y* and *Z* spectra from identical crystal slabs, (100) sections 80 μm thick were prepared. They were heated at 350 °C and 2–2.5 kbar for 14 d. The resulting exchange of ~50% was rather disappointing, the inner 30 μm of one slab yielding only ~25% exchange. These results clearly indicate that the H-diffusion rate along [001] (the *Z* direction) is at least one order of magnitude faster than it is along [100] (the *X* direction). Exact H-diffusion coefficients are not given because the crystals with many fissures did not allow for pure surface-diffusion studies. Nevertheless, the results are easily reconciled with the lawsonite structure. Even though the structure contains large channels along [100] (Fig. 1), these channels are rather narrow (those contain-

ing the hydroxyl H atoms) or obstructed by Ca atoms. In contrast, there exist large channels parallel to [001], which contain the H atoms of the hydroxyl groups and H₂O molecules at their center.

The isotopically diluted Y spectra of lawsonite (Fig. 3) are almost identical to the undiluted Y spectra (i.e., all bands are retained, and band widths and peak positions are almost unchanged). Thus, it seems that the different structural environments of the H atoms (at least in the low-temperature phases) prevent extensive band coupling. However, the band heights of the high-energy bands, and the low-temperature frequency of the low-energy band in the Y spectrum are somewhat different, as discussed below.

DISCUSSION

The symmetry of the H₂O molecule

Prior to a detailed band assignment (see below) the vibrational behavior of an H₂O molecule in a crystal must be elucidated. Previous papers on IR spectroscopy of H₂O in minerals showed that the H₂O molecule can be treated as an almost free, symmetric molecule (symmetry $mm2 = C_{2v}$) in minerals such as cordierite (Goldman et al. 1977) and beryl (Wood and Nassau 1967). According to group theory (e.g., Cotton 1990), two modes behave as A₁ species and one behaves as B₁ or B₂ species (according to the setting). In other words, there occur a symmetric stretching mode (ν_1) and a bending mode (ν_2), which are polarized parallel to the axis of the molecule, and an asymmetric stretching mode (ν_3), which is polarized perpendicular to the former and parallel to the plane of the molecule. It is important to realize that the symmetric and asymmetric stretching modes (separated by ~ 100 cm⁻¹ in H₂O gas) are normal modes of both symmetrically equivalent H atoms, the polarization properties of which are established by addition or subtraction of the vectors of the single O-H vibrations.

However, analysis of the lawsonite spectra according to the assumed behavior, discussed above, of the H₂O molecule in a crystal does not result in successful and consistent band assignment. Even though Labotka and Rossman (1974) presented a band assignment that was based on this assumption (two low-energy H₂O bands, ν_1 and ν_3 , and a split, high-energy O-H stretching band) and was consistent with the room-temperature structure of lawsonite available at that time, this model is not in agreement with our present knowledge of the low-temperature orientations of the hydroxyl and H₂O groups and their different hydrogen bonds to neighboring O atoms.

When the H atoms of the H₂O molecule become nonequivalent, the symmetry of the molecule is reduced to $m (= C_s)$. The former B species is no longer valid, and two single stretching modes appear at the expense of the former ν_1 and ν_3 modes. This behavior is well documented in HDO and HDO-containing crystalline hydrates, which show the single O-H and O-D stretching modes

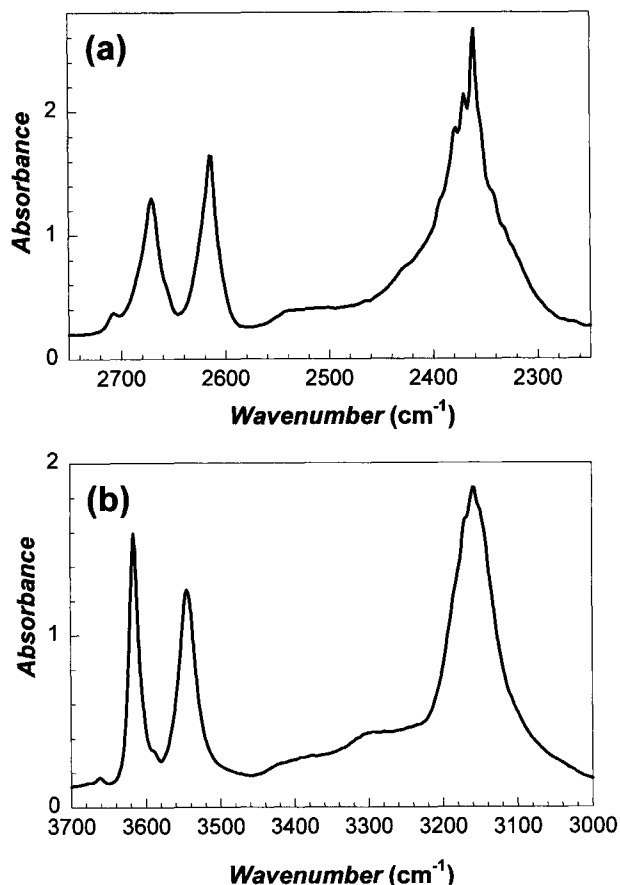
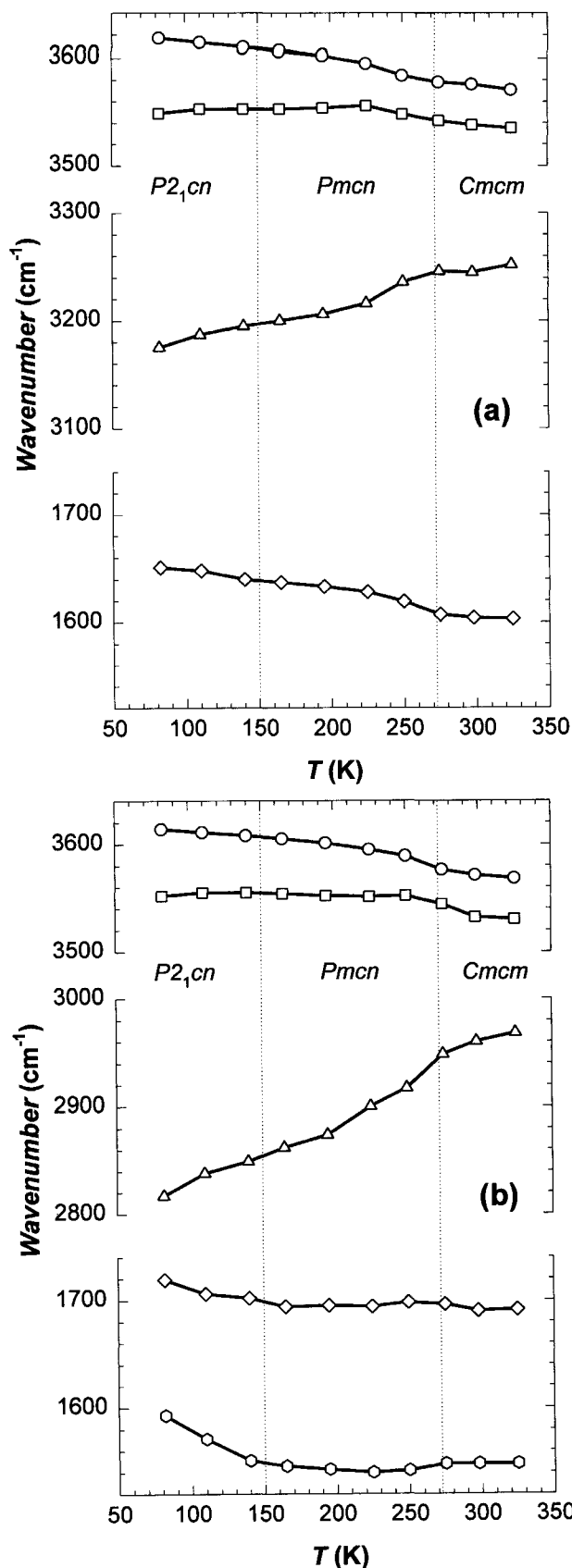


FIGURE 3. The Y spectra of deuterated lawsonite at 82 K. (a) O-D stretching frequencies in a 30 μm (100) slab with $\sim 25\%$ D₂O. (b) O-H stretching frequencies in a 20 μm (001) slab with $\sim 80\%$ D₂O. The tiny spikes on top of the low-energy peaks represent noise enhanced by the strong absorbance.

(separated by ~ 800 – 900 cm⁻¹) and the H-O-D bending mode (Franks 1973). Because both nonequivalent masses (as in HDO) and nonequivalent O-H force constants (i.e., bond strengths and lengths) cause considerable changes in the band frequencies (note that frequency squared is proportional to force constant divided by reduced mass), it is evident that the H₂O molecule in lawsonite (possessing two differently bonded H atoms) can no longer be regarded as a free molecule with C_{2v} symmetry. Moreover, it will be shown in the final band assignment that the separation of the two O-H stretching modes of the H₂O molecule by 600–800 cm⁻¹ (increasing with decreasing temperature, Fig. 4b) is almost as great as that of the O-H and O-D modes in an HDO molecule. In addition, the similarity between the deuterated and undeuterated lawsonite spectra also shows that, because of the different hydrogen bonds, the vibration of each OH group is independent of the other. Hence, the band assignment employs single O-H vectors instead of ν_1 and ν_3 H₂O stretching modes arising from simultaneous, coupled motions of both equivalent H atoms.



Band assignment

Two features are used for the band assignment in the following discussion. (1) The band intensities of polarized spectra provide geometric information on possible O-H vector orientations. This method has been used in previous investigations to discover the orientation of H₂O and hydroxyl groups in hydrous minerals (e.g., Labotka and Rossman 1974) and to propose sites of H incorporation in nominally anhydrous minerals (e.g., Beran 1987; Libowitzky and Beran 1995). (2) The band frequencies provide information on the strengths and lengths of hydrogen bonds. Generally, the shorter and stronger the hydrogen bond, the lower is the frequency of the O-H stretching band. Compilations of band frequencies vs. hydrogen-bond lengths in solid materials were published by Nakamoto et al. (1955), Franks (1973), Novak (1974), and Mikenda (1986). Even though these correlations show considerable scatter, they allow one to predict approximate hydrogen-bond distances from frequencies and vice versa.

The band assignment was performed with 110 K spectra, because bands are sharp and clearly discernible at these low temperatures, and H-atom positions and bond distances are least distorted by librational motions in the 110 K *P2₁cn* lawsonite structure. The band frequencies vs. temperature are shown in Figure 4. The different hydrogen-bond distances and their evolution with temperature are presented in Table 1 and Figure 5.

The lowest energy O-H stretching band occurs predominantly in the Z spectrum at 2838 cm⁻¹ and indicates an orientation of the O-H vector almost parallel to [001]. Figure 1c shows that only the O5-Hw vector of the H₂O molecule is aligned in this direction. The slight deviation of ~15° from the [001] direction may be responsible for the weak and very broad component near 2800–2900 cm⁻¹ in the Y spectrum. However, this cannot be proved because of overlapping, weak, low-frequency interference fringes. Because its frequency is the lowest one observed in lawsonite, the corresponding hydrogen bond must also be the shortest. Table 1 and Figure 5 show that the Hw...O4 and O5-Hw...O4 distances are the shortest ones in the hydrogen-bond system of lawsonite. According to the diagrams of Mikenda (1986) an O-H...O distance of ~2.60 Å and an H...O distance of ~1.60–1.65 Å (unfortunately, the latter diagram is poorly defined toward strong hydrogen bonds) correspond to 2838 cm⁻¹. This is in excellent agreement with the observed hydrogen-bond distances of 2.599 and 1.66 Å in the low-temperature structure of lawsonite and confirms the proposed band assignment.

The other low-energy band that occurs predominantly in the Y spectrum at 3187 cm⁻¹ indicates a preferred O-H

FIGURE 4. Wavenumber vs. temperature plot of the stretching and bending frequencies in lawsonite. (a) Y spectra. (b) Z spectra.

vector alignment parallel to [010]. Figure 1c shows that the hydroxyl O4-Hh vector is the best choice. The slight misalignment (deviation of 12° toward Z) may be responsible for the very weak component near 3200 cm^{-1} in the Z spectra. Table 1 and Figure 5 confirm that the second-strongest hydrogen bond corresponds to the Hh atom of one hydroxyl group. According to the diagrams of Mikenda (1986), 3187 cm^{-1} corresponds to an O-H \cdots O distance of $\sim 2.72\text{ \AA}$ and an H \cdots O distance of $\sim 1.75\text{ \AA}$. This is in good agreement with the values of 2.660 and 1.74 \AA for the O4-Hh \cdots O4a and Hh \cdots O4a bonds, respectively, in the 110 K structure of lawsonite. The additional, very weak Hh \cdots O2 bonds (if they are considered as hydrogen bonds at all) with distances as great as $2.3\text{--}2.4\text{ \AA}$ seem to have no influence on the strength and band frequency of the O4-Hh bond.

The two high-energy stretching bands that occur with almost equal intensities in the Y and Z spectra are undoubtedly caused by the two remaining Hwa and Hha atoms. The intermediate orientations (toward Y and Z) of the O5-Hwa ($\sim 30^\circ$) and O4a-Hha ($\sim 42^\circ$) vectors are in approximate agreement with the almost equal intensities in Y and Z. However, the assignment of the individual peaks is more difficult, because both peaks are separated by only $60\text{--}70\text{ cm}^{-1}$, and because both peaks show a multiple, weak hydrogen-bond scheme.

Table 1 and Figure 5a indicate that the weakly bonded Hha atom of the hydroxyl group shows considerably stronger hydrogen bonds (Hha \cdots O2a = 2.04 \AA , Hha \cdots O5 = 2.14 \AA) than the weakly bonded Hwa atom of the H₂O molecule (Hwa \cdots O2 = 2.20 \AA , Hwa \cdots O4a = 2.41 \AA). This is also supported by the corresponding O-H \cdots O distances in Figure 5b. Consequently, the band at $\sim 3554\text{ cm}^{-1}$ is assigned to the stretching frequency of the O4a-Hh hydroxyl group, and that at $\sim 3612\text{ cm}^{-1}$ to the O5-Hwa stretching frequency of the H₂O molecule. According to the diagrams of Mikenda (1986) these frequencies correspond to O-H \cdots O distances of 3.08 and $>3.2\text{ \AA}$, and H \cdots O distances of 2.15 and $>2.25\text{ \AA}$. These values are considerably higher than the observed values. One reason for this difference may be that the correlations of Mikenda (1986) are defined by only a few scattered data points at the high-energy end of the diagrams. Another reason may be that these literature data contain only the best-defined, straight hydrogen bonds, whereas the weakly bonded Hwa and Hha atoms of the low-temperature lawsonite structure show strongly bent and bifurcated hydrogen bonds. The O-H \cdots O distances of 2.96 and 3.05 \AA were obtained using the diagram of Nakamoto et al. (1955), which is defined up to almost 3700 cm^{-1} . These results fit somewhat better to the observed distances in the 110 K lawsonite structure. However, because of the steep slope of the correlation diagram, uncertainties of at least $\pm 0.05\text{ \AA}$ must be considered. Nakamoto et al. (1955) also showed that strongly bent hydrogen bonds diverge from the best-fit curve. Unfortunately, their study lacks pure H \cdots O data. Nevertheless, a rough estimate (using the above distances from the low-

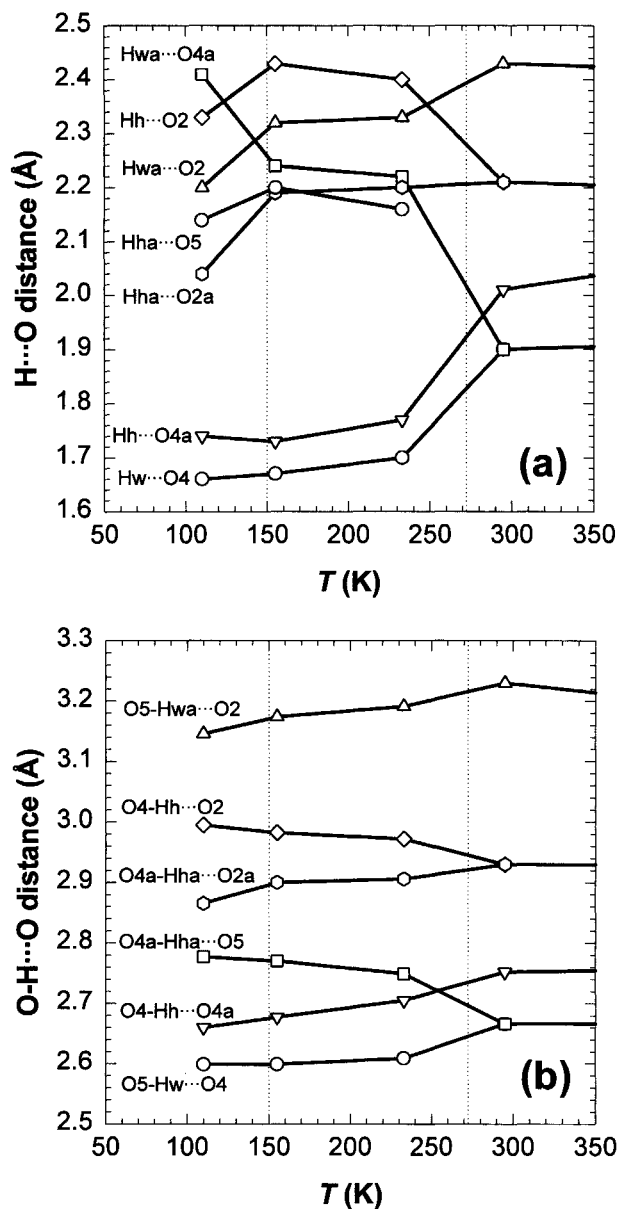


FIGURE 5. Plot of hydrogen-bond distances in lawsonite (values from Table 1) vs. temperature. (a) H \cdots O distances. (b) O-H \cdots O straight distances.

energy bands) yields O \cdots H distances of 2.01 and 2.10 \AA , which are in reasonable agreement with the Hha \cdots O2a and Hwa \cdots O2 distances of 2.04 and 2.20 \AA .

Closer examination of the exact intensities of the high-energy bands in the Y and Z spectra (when normalized for a thickness of $4\text{ }\mu\text{m}$) confirms the band assignment. At 110 K , the 3612 cm^{-1} band has a band area of 72 cm^{-1} in Y and 61 cm^{-1} in Z. Hence, the O-H vector should deviate from the 45° alignment toward Y. This is actually verified in Figure 1c for the O5-Hwa vector ($\sim 30^\circ$ to [010]). The 3554 cm^{-1} band has a band area of 35 cm^{-1} in Y and 35 cm^{-1} in Z. Hence, the resulting O-H

vector should be very close to 45°, and this is confirmed in Figure 1c for the O4a-Hha vector (with ~42° to [001]).

A controversial assignment of the high-energy bands is obtained if the (bending + stretching) combination mode of the H₂O molecule is investigated. This band at 5180 cm⁻¹ is most intense in the Z spectrum. If the H₂O bending mode of the Y spectrum at ~1650 cm⁻¹ is subtracted from the combination frequency, the resulting stretching frequency of 3530 cm⁻¹ is close to the observed frequency, 3554 cm⁻¹. However, if the same calculation is performed for the 1570 cm⁻¹ bending mode in the Z spectrum, the expected stretching frequency of 3610 cm⁻¹ is much closer to the observed 3612 cm⁻¹ band than in the former case. In contrast to these considerations, it must be argued that, if normal mode analysis (factor-group analysis in a crystal) and group theory (e.g., Cotton 1990) are used, all binary combinations of IR-active modes result in IR-forbidden modes in a centrosymmetric lattice (e.g., *Pmcn*, factor group *D_{2h}*). However, if we combine the Raman-active H₂O bending mode (species A_g) at 1578 cm⁻¹ (Le Cléac'h and Gillet 1990) with the high-energy H₂O stretching mode in Z (species B_{1u}, according to their setting) we obtain an IR-active combination mode in Z. This combination also favors the assignment of the 3612 cm⁻¹ band to the H₂O molecule. Because the latter also agrees with all results from geometric and frequency vs. hydrogen-bond-length considerations, the assignment of the 3612 cm⁻¹ band to O5-Hwa and the 3555 cm⁻¹ band to O4a-Hha is considered safe.

The weak, split band at 4352–4416 cm⁻¹ in the X spectra of lawsonite may be interpreted as a metal-OH frequency (Rossman 1988), i.e., the combination of M-O and O-H stretching modes. This band, which shows an almost identical amount of peak splitting at low temperatures as the high-energy O-H stretching bands at 3554–3612 cm⁻¹, confirms the participation of the O5-Hwa and O4a-Hha stretching frequencies in a combination mode. The remaining component of this combination should have a wavenumber of about 800 cm⁻¹. As discussed above (using group theory), a possible candidate for this combination cannot be found in the IR-active modes. Nevertheless, it was observed in the polarized Raman spectrum of lawsonite by Le Cléac'h and Gillet (1990) at 809 cm⁻¹ (Al-O₆ vibration was assumed), belonging to species B_{1g} or B_{3g} (according to their setting). In combination with the high-energy O-H stretching modes (both species B_{3u} and B_{1u} in their setting) the resulting band(s) must belong to species B_{2u} (in their setting), which actually represents the X polarization in the present paper.

Spectral evolution and phase transitions

Figure 2 shows that the IR spectra change smoothly in the temperature range 82–325 K. Only the appearance or disappearance of peak splitting in the high-energy O-H stretching bands and in the bands near 4400 cm⁻¹ seems to perturb the impression of continuous changes. However, as the wavenumber vs. temperature plots in Figure

4 show, even the apparently unsplit high-energy band at ambient temperatures is composed of two constituents (as revealed by peak fitting).

This continuous spectral evolution contradicts the behavior expected from displacive phase transition, altering the highly symmetric H₂O and hydroxyl positions in Figure 1a (one hydroxyl Hh atom and one H₂O Hw atom in the *Cmcm* structure) to the asymmetric positions in Figures 1b and 1c (one Hh, one Hha, one Hw, and one Hwa atom in the *Pmcn* and *P2₁cn* structures). The lowering of symmetry (especially during the 273 K *Cmcm*-*Pmcn* transition) should lead to a strong change in the appearance of the spectra near 273 K. Figure 1 and Table 1, showing sudden transitional changes in the H₂O and hydroxyl coordination spheres (represented by bond lengths and angles), also suggest a nonlinear behavior of frequency vs. temperature plots. The evolution of the band positions with relation to the hydrogen-bond distances from low to ambient temperatures is examined below.

The correlation of the 110 K hydrogen bonds with the O-H stretching frequencies was discussed in the preceding description of the band assignment. At 155 K (above the *P2₁cn*-*Pmcn* phase boundary) the low-energy stretching bands appear at slightly higher frequencies than at 110 K [2860 (Z) and 3200 cm⁻¹ (Y)]. The corresponding H···O (O-H···O) bond distances from the diagrams of Mikenda (1986) are ~1.60–1.65 (~2.60) and 1.75 (2.72) Å. These values (even if not well defined for the short bond lengths) are in good agreement with the values of 1.67 (2.60) and 1.73 (2.68) Å from Table 1 or from the graphs in Figure 5. The frequencies of the high-energy bands are almost unchanged from 110 to 155 K and, thus, are not reconsidered. Note, however, that because of the higher symmetry in *Pmcn* the bonds to O2 (and O2a) are doubled, thus forming symmetric, bifurcated hydrogen bonds (Table 1).

At 233 K the low-energy stretching bands appear at 2910 (Z) and 3225 cm⁻¹ (Y). The corresponding H···O (O-H···O) distances from the diagrams of Mikenda (1986) are ~1.62–1.67 (~2.61) and 1.76 (2.74) Å. They are in good agreement with those of 1.70 (2.61) and 1.77 (2.71) Å from Table 1 and Figure 5. The high-energy bands are at 3550 and 3590 cm⁻¹; the former is almost identical to the 110 K value. The corresponding H···O-bond lengths of 2.17 (Hha···O5) and 2.21 Å (Hwa···O4a) are in good agreement with the observed values of 2.16 and 2.22 Å from Table 1 and Figure 5. Because of the bent and bifurcated bonds the O-H···O values cannot be reasonably correlated, and even the coincidence of the H···O bonds may be incidental.

In the *Cmcm* structure of lawsonite at 295–298 K the stretching frequencies of the low-energy bands occur at 2960 (Z) and 3245 cm⁻¹ (Y). The corresponding H···O (O-H···O) distances are ~1.65–1.70 (2.63) and 1.79 (2.75) Å. The O-H···O distances are in good agreement with the observed values of 2.67 and 2.75 Å (between the rigid "hinges" of the hydrogen bonds). In contrast, the observed O···H distances of 1.90 and 2.01 Å (Table

1) disagree with the observed low-energy bands. Moreover, the high space group symmetry should result in only one hydroxyl stretching frequency and only two closely spaced (symmetric and asymmetric) stretching frequencies of the H₂O molecule. Nevertheless, Figure 4 shows that the four-band character of the spectrum is conserved across the 273 K phase boundary, continuing the uniform shift of stretching frequencies. The slopes of the wavenumber vs. temperature plots are slightly different only on the low- and high-temperature sides of the *Pmcn*-*Cmcm* transition.

This behavior provides strong evidence that the 273 K phase transition from the less symmetric *Pmcn* to the highly symmetric *Cmcm* structure of lawsonite at ambient temperatures is not caused by the rotation of hydroxyl groups and H₂O molecules to static, symmetric positions, as drawn in Figure 1a, but rather by the dynamically and disordered occupation of hydroxyl and H₂O sites around the highly symmetric positions of Figure 1a. The single H sites of this dynamic disorder (or the end-points of these librational motions) are probably very similar to the positions occupied in the low-temperature structures of lawsonite. This is supported by the continuous shifts of the stretching frequencies across the phase boundaries (as described above) and by the unchanged, exclusive appearance of the low-energy stretching bands in either the *Y* or *Z* spectra at ambient temperatures. The latter can be reconciled only with H-atom positions of the low-temperature structures rather than with those from the room-temperature structure. In addition, preliminary results of a room-temperature, single-crystal NMR study also indicated a disordered H sublattice in lawsonite, the single H sites being close to those of the low-temperature *Pmcn* structure (S.P. Gabuda and S.G. Kozlova, personal communication).

The librational motion of the hydroxyl and H₂O groups is also indicated by the anisotropic displacement parameters (ADPs) of the H atoms and indirectly by the overly short O-H bonds observed in both X-ray and neutron refinements. Refinements of the X-ray data of Libowitzky and Armbruster (1995) and of a first neutron data set at room temperature (George Lager, personal communication) revealed that the Hh atoms show an extremely strong ADP along [001], which is in agreement with the Hh libration around the O4 atoms mostly within the (100) plane. The neutron data also showed the librational motion of the Hw atoms by strong displacement along *Y* and *Z* (thus pointing or vibrating toward Hw sites of the low-temperature phases), whereas the X-ray data suggested a preferred displacement parallel to [100], which is also exhibited by the O5 atom of the H₂O molecule (Libowitzky and Armbruster 1995).

Deuterated samples

The 82 K O-D stretching bands of the *Y* spectrum of a 30 μm thick (100) lawsonite slab with $\sim 25\%$ D₂O are shown in Figure 3a. The corresponding 82 K O-H stretching bands in the *Y* spectrum of a 20 μm thick (001)

slab with $\sim 80\%$ D₂O are presented in Figure 3b. The two spectra are almost identical in appearance, even their intensities (comparing band areas instead of amplitudes) are comparable. Slight intensity differences may be attributed to slightly different incorporation of D in the hydroxyl groups and H₂O molecules. Comparison of Figure 3b with the pure 82 K *Y* spectrum in Figure 2b shows that the general appearance of the bands is almost identical. This fact, together with the nearly constant band widths, indicates that band-coupling effects must be weak in lawsonite. This is consistent with the different stretching frequencies of the four H atoms, which make coupling unlikely. This also explains why [similar to isotopically diluted samples (Franks 1973)] symmetric and asymmetric stretching modes of the H₂O molecule, involving coupled motions of the two O-H bonds, are disabled. However, two features appear slightly changed. (1) The low-energy band of the $\sim 80\%$ deuterated sample shifts to somewhat lower energy at 3160 cm^{-1} in comparison with that of the pure hydrogenated sample at 3175 cm^{-1} . This feature is observed in the whole temperature range investigated. (2) The intensity ratio between the two high-energy bands changes from $\sim 2:1$ in the pure H lawsonite sample to $\sim 1:1$ in the deuterated samples at 82 K. Feature 1 is easily explained by the influence of the D atoms. Because $\sim 80\%$ of the H atoms are replaced by D atoms in the spectrum of Figure 3b, slightly changed frequencies must be expected (especially for the Hh atom, which, by the strong Hh...O4a bond, has a weaker O4-H bond). The second feature may be explained by a similar effect. The high concentration of D atoms may lead to slightly rotated Hhw and Hha positions. Thus, the changed geometry would change the intensity ratios between *Y* and *Z* spectra. Unfortunately, reliable *Z* spectra could not be obtained, because the high-energy O-D stretching bands interfere with the strong, lowest-energy O-H band, and because the slow diffusion rates vertical to *Z* impede the study of isotopically diluted, high-energy O-H bands in *Z* spectra. Another explanation for feature 2 might be, that, contrary to the general impression, slight band coupling causes the 2:1 intensity ratio in the pure H lawsonite samples. Finally, loss of H atoms from the most weakly hydrogen-bonded Hha sites during the deuteration experiments close to the stability limits of lawsonite may also account for the change of the band intensities.

Band intensities

Lawsonite has a density (*D*) of 3.1 g/cm^3 and stoichiometrically contains 11.5 wt% H₂O. Because the four stretching bands are well separated (at least at low temperatures), and because each stretching band can be clearly assigned to a certain O-H vibration, an H₂O content of 2.87 wt% was correlated with the intensities of each of the four stretching bands. Because peak heights change strongly with temperature (Fig. 2), and because high-energy bands are usually higher and sharper than low-energy peaks at low wavenumbers (Nakamoto et al. 1955), the band areas (i.e., the "integrated absorbances," *A_i*) were

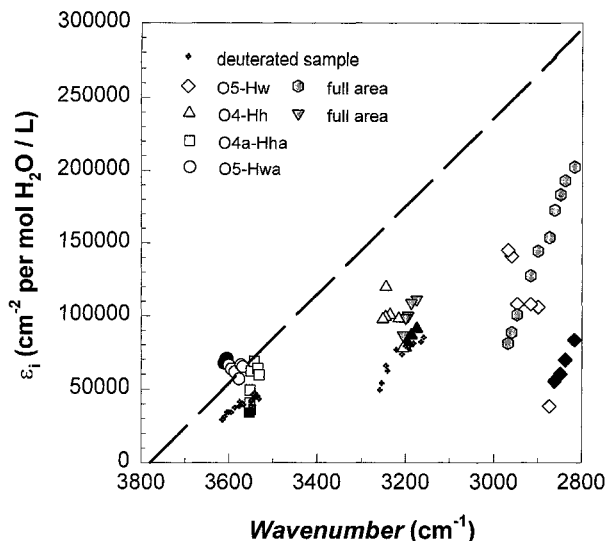


FIGURE 6. Integrated molar absorptivity coefficients vs. wavenumber of lawsonite stretching bands. Solid symbols represent values from the spectra at the four lowest temperatures. Shaded symbols indicate intensities from the full band area (instead of the main Voigt curve during peak fitting) of the broad low-energy bands. Values from the 20 μm slab with $\sim 80\%$ D_2O are indicated by crosses. The broken line represents the trend of Paterson (1982). Note that Paterson (1982) used "mol H" instead of "mol H_2O ."

considered representative for the intensities. According to Libowitzky and Rossman (1996), the band intensities of the three polarization directions must be added to obtain the effective intensity (parallel to the absorber). Because the X direction shows only negligible intensities in lawsonite, only Y and Z were summed up. The band intensity, sample thickness (t), and H_2O concentration (c) are related by the Beer-Lambert law, which, in the form of Beran et al. (1993), is written as c (wt% H_2O) = A_i (cm^{-1}) $\cdot 1.8/[t$ (cm) $\cdot D$ (g/cm^3) $\cdot \epsilon_i$ (cm^{-2} per mol $\text{H}_2\text{O}/\text{L}$)], where ϵ_i is the integral (or integrated) molar absorption coefficient. The factor 1.8 results from the conversion of the H_2O concentration from mole per liter to weight percent. Because the H_2O concentration corresponding to every single band is known (as are t and A_i), the ϵ_i values were calculated for every band at all temperatures. Figure 6 gives the resulting plot of ϵ_i vs. wavenumber.

The general trend of Paterson (1982) is confirmed by the broken line in Figure 6, which shows increasing ϵ_i values with decreasing wavenumbers as a result of decreasing bond strength and easier polarizability of O-H bonds with enhanced $\text{H}\cdots\text{O}$ bonding. However, the present data suggest a lower wavenumber dependence of ϵ_i than Paterson's trend, which is also in agreement with recent results on other hydrous minerals (Libowitzky and Rossman, in preparation). The plot also shows that the values from the low-temperature spectra (solid symbols) have less scatter than those from the high-temperature spectra because of the easier and more accurate peak fitting of the well-discerned bands. However, two points of

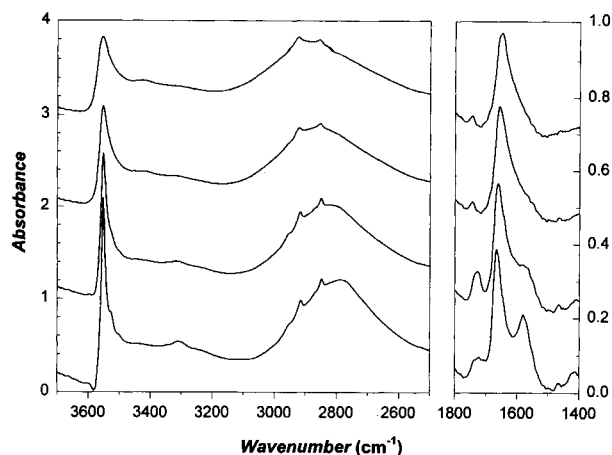


FIGURE 7. FTIR spectra of a hennomartinite KBr pellet at 82 (bottom), 195, 298, and 373 K (top). Spectra are vertically offset. The spikes at 2850 and 2920 cm^{-1} are organic impurities.

deviation from the trend are visible in the plot. (1) The highest energy Hwa bands give values about twice as high as the other high-energy bands. (2) The lowest energy Hw bands show considerable scatter. The latter observation is easily explained by inaccurate peak fitting because only one symmetric Voigt curve was used for the band-area calculation, even if (owing to the highly asymmetric band shape) a second or third band had to be used for an accurate fit. The very broad band was also highly sensitive to correct background selection. The reason for the difference between the highest energy bands (1) is not clear. The difference may be caused by a form of band coupling, which is supported by the fact that the deuterated samples (crosses in Fig. 6) do not show this effect at all (this was already discussed above). Another possible explanation is that, for some poorly understood reason, the Hwa position is more occupied than some other site (not necessarily in terms of higher site abundance, but, because all processes occur dynamically, in terms of time).

Comparison with the FTIR spectrum of hennomartinite

Recently, Libowitzky and Armbruster (1996) found that hennomartinite, $\text{SrMn}_2[\text{Si}_2\text{O}_7](\text{OH})_2 \cdot \text{H}_2\text{O}$, a mineral of the lawsonite type, shows phase transitions similar to those of lawsonite. However, owing to the expanded lattice parameters, the transitions occur at elevated temperatures, and a complicated disorder-twin evolution and a probably monoclinic distortion at ambient temperatures occurs. Nevertheless, as in lawsonite, the transitions from high to ambient temperatures were shown to be predominantly caused by the rotation of OH and H_2O groups to form strong hydrogen bonds. Thus, one H atom of the H_2O molecules and one H atom of the hydroxyl groups show short, strong hydrogen bonds ($\text{O}-\text{H}\cdots\text{O} \approx 2.6\text{--}2.7$ Å), whereas every other H atom shows very weak or negligible hydrogen bonding ($\text{O}-\text{H}\cdots\text{O} > 3.0$ Å).

The FTIR spectra of a hennomartinite KBr pellet between 82 and 373 K are shown in Figure 7. (Because of

the extremely small size of the crystals and intergrown crystal aggregates, a polarized FTIR study on oriented single-crystal slabs was not feasible.) There are two bands in the O-H stretching region, and one (two at low temperatures) in the H₂O bending region. The sharp O-H stretching band at 3550 cm⁻¹ is correlated with the weakly bonded H atoms in hennomartinite. The intense broad band near 2800–2900 cm⁻¹ is assigned to the strongly bonded H atoms. Even though the spectra show strong similarities to those of lawsonite (obviously caused by the similar grouping of bands owing to weakly and strongly hydrogen-bonded H atoms), there are two main differences. (1) There is only one high-energy and only one low-energy band in hennomartinite, whereas lawsonite has two of each. This feature might be explained by an exact overlap of the high-energy bands and by very similar positions of the low-energy bands (the broad band in hennomartinite is much wider and more intense than that of the lawsonite Z spectrum). However, because of the unpolarized spectra, information on the single decomposed band and on the geometric situation could not be obtained. (2) The temperature shift of peak positions in the hennomartinite spectra is weak in comparison with that of lawsonite. The high-energy band remains constant within the temperature range investigated, and the low-energy band decreases by only 80–90 cm⁻¹ from 373 to 82 K (in comparison with ~200 cm⁻¹ from 325 to 82 K in lawsonite). The strong bending mode at 1650 cm⁻¹ is also almost temperature independent. This is in good agreement with the ambient temperature structure of hennomartinite (stable up to ~370 K), which is comparable to that of lawsonite below 150 K. Thus, the hydrogen bonds have already settled, and only the strong hydrogen bonds are further enhanced due to reduced thermal vibration. This is also confirmed by the 3550, 2800, and 1650 cm⁻¹ band positions of hennomartinite (Fig. 7), which are equal to the low-temperature lawsonite band positions. A very weak combination mode near 5180 cm⁻¹ shows that the weakly bonded H atom of the H₂O molecule is also engaged in the high-energy stretching mode.

ACKNOWLEDGMENTS

The authors thank P. Wyllie (California Institute of Technology) for the use of his cold-seal equipment, and J. Eiler (California Institute of Technology) for technical help with the cold-seal vessels. G.A. Lager (University of Louisville) provided information on the results of his neutron refinement of lawsonite at room temperature, and S.P. Gabuda and S.G. Kozlova (Novosibirsk) provided preliminary data on a single-crystal proton NMR study of lawsonite at room temperature. The comments of referees H. Cynn (UCLA) and C. Merzbacher (Naval Research Laboratories), as well as the remarks of Associate Editor A. Hofmeister helped to improve the quality of the manuscript. E.L. appreciates financial support from the Fonds zur Förderung der wissenschaftlichen Forschung, Austria, during an Erwin-Schrödinger fellowship, project J01098-GEO. G.R.R. acknowledges support from the National Science Foundation, grant EAR-9218980. This paper represents the Division of Geological and Planetary Sciences of the California Institute of Technology, contribution 5623.

REFERENCES CITED

- Baur, W.H. (1978) Crystal structure refinement of lawsonite. *American Mineralogist*, 63, 311–315.
- Beran, A. (1987) OH groups in nominally anhydrous framework structures: An infrared spectroscopic investigation of danburite and labradorite. *Physics and Chemistry of Minerals*, 14, 441–445.
- Beran, A., Langer, K., and Andrut, M. (1993) Single crystal infrared spectra in the range of OH fundamentals of paragenetic garnet, omphacite and kyanite in an eklogitic mantle xenolith. *Mineralogy and Petrology*, 48, 257–268.
- Comodi, P., and Zanazzi, P.F. (1996) Effects of temperature and pressure on the structure of lawsonite. *American Mineralogist*, 81, 833–841.
- Cotton, F.A. (1990) *Chemical applications of group theory* (3rd edition), 461 p. Wiley, New York.
- Franks, F., Ed. (1973) *Water: A comprehensive treatise*, vol. 2, 684 p. Plenum, New York.
- Goldman, D.S., Rossman, G.R., and Dollase, W.A. (1977) Channel constituents in cordierite. *American Mineralogist*, 62, 1144–1157.
- Labotka, T.C., and Rossman, G.R. (1974) The infrared pleochroism of lawsonite: The orientation of the water and hydroxide groups. *American Mineralogist*, 59, 799–806.
- Lager, G.A., Armbruster, T., and Faber, J. (1987) Neutron and X-ray diffraction study of hydrogarnet Ca₃Al₂(O₄H₄). *American Mineralogist*, 72, 756–765.
- Le Cléac'h, A., and Gillet, P. (1990) IR and Raman spectroscopic study of natural lawsonite. *European Journal of Mineralogy*, 2, 43–53.
- Libowitzky, E., and Armbruster, T. (1995) Low-temperature phase transitions and the role of hydrogen bonds in lawsonite. *American Mineralogist*, 80, 1277–1285.
- Libowitzky, E., and Beran, A. (1995) OH defects in forsterite. *Physics and Chemistry of Minerals*, 22, 387–392.
- Libowitzky, E., and Armbruster, T. (1996) Lawsonite-type phase transitions in hennomartinite, SrMn₂[Si₂O₇](OH)₂·H₂O. *American Mineralogist*, 81, 9–18.
- Libowitzky, E., and Rossman, G.R. (1996) Principles of quantitative absorbance measurements in anisotropic crystals. *Physics and Chemistry of Minerals*, 23, 319–327.
- Mikenda, W. (1986) Stretching frequency versus bond distance correlation of O-D(H)···Y (Y = N, O, S, Se, Cl, Br, I) hydrogen bonds in solid hydrates. *Journal of Molecular Structure*, 147, 1–15.
- Nakamoto, K., Margoshes, M., and Rundle, R.E. (1955) Stretching frequencies as a function of distances in hydrogen bonds. *Journal of the American Chemical Society*, 77, 6480–6486.
- Newton, R.C., and Kennedy, G.C. (1963) Some equilibrium reactions in the join CaAl₂Si₂O₈-H₂O. *Journal of Geophysical Research*, 68, 2967–2983.
- Novak, A. (1974) Hydrogen bonding in solids: Correlation of spectroscopic and crystallographic data. *Structure and Bonding*, 18, 177–216.
- Paterson, M.S. (1982) The determination of hydroxyl by infrared absorption in quartz, silicate glasses and similar materials. *Bulletin de Minéralogie*, 105, 20–29.
- Pawley, A.R. (1994) The pressure and temperature stability limits of lawsonite: Implications for H₂O recycling in subduction zones. *Contributions to Mineralogy and Petrology*, 118, 99–108.
- Rossman, G.R. (1988) Vibrational spectroscopy of hydrous components. In *Mineralogical Society of America Reviews in Mineralogy*, 18, 193–206.
- Sunshine, J.M., Pieters, C.M., and Pratt, S.F. (1990) Deconvolution of mineral absorption bands: An improved approach. *Journal of Geophysical Research*, 95(B5), 6955–6966.
- Wickman, F.E. (1947) The crystal structure of lawsonite, CaAl₂(Si₂O₇)(OH)₂·H₂O. *Arkiv för Kemi Mineralogi och Geologi*, 25A, 1–7.
- Wood, D.L., and Nassau, K. (1967) Infrared spectrum of foreign molecules in beryl. *Journal of Chemical Physics*, 47, 2220–2228.

MANUSCRIPT RECEIVED DECEMBER 1, 1995

MANUSCRIPT ACCEPTED MAY 28, 1996